ENHANCED SCATTERING DIAGNOSTICS ON A TOKAMAK-LIKE PLASMA

E.Z. Gusakov, N.M. Kaganskaya, **M. Krämer***, P. Morcinczyk* and V.L. Selenin

Ioffe Physico-Technical Institute, St. Petersburg, Russia
**Experimentalphysik II, Ruhr-Universität Bochum, Germany*

Abstract. The first application of the Interferometer Enhanced Scattering (IES) technique for investigating lower hybrid (LH) waves in tokamak-like plasma geometry is reported. Reasonable agreement of the LH density perturbations measured by IES and RF probe techniques is shown.

During the last decade, the enhancement of the scattering cross section of electromagnetic waves in the vicinity of a hybrid resonance was widely used to diagnose fluctuations and waves in magnetized plasmas [1]. The Enhanced Scattering (ES) diagnostic based on this effect has a high sensitivity to small-scale fluctuations and a good spatial resolution. The probing is carried out by microwaves with a vacuum wavelength much larger than the wavelength of the fluctuations. A weakness of the ES diagnostic is the poor wavenumber resolution caused by the rapid increase of the probing wavenumber near the hybrid resonance. Two modifications of the ES diagnostic combining its benefits with a reasonable wavenumber resolution were proposed recently: 1. The RADAR ES diagnostic makes use of the fact that the time delay of the signal backscattered in the hybrid resonance scales linearly with the fluctuation wavenumber [2]. 2. The Correlative or Interferometer ES utilizes the dependence of the backscattered signal A_{ES} on the phase of the fluctuation in the hybrid resonance point [3,4]. According to [4], the backscattered signal in the case of single antenna operation is given by the expression

$$A_{ES}(t,x_r)=\frac{i\,\omega_i\,A_i}{16}\int\frac{d\Omega d^3\vec{q}dk_{iy}dk_{iz}}{(2\pi)^6}\frac{\delta n_{\Omega,\vec{q}}}{n_e}e^{i\Omega t-iqx_r(\omega_i)-iq_Zz_i-iq_yy_i}f(k_{iy},k_{iz})f(q_y-k_{iy},q_z-k_{iz})\Theta I(\vec{q}) \quad , \qquad (1)$$

where $|A_{ES}|^2$ and $|A_i|^2$ are the scattered and incident powers at the antenna, $\delta n_{\Omega,q}$ is the spectral Fourier harmonic of the electron density fluctuation, q and q_z are the components of the fluctuation wavenumber in direction of the plasma inhomogeneity and the magnetic field strength, and q_y is the remaining component, $f(k_{iy},k_{iz})$ is the incident and receiving antenna pattern, y_i and z_i are the antenna coordinates, Θ is the fraction of the incident wave energy absorbed in the resonance, and the standard factor I(q) is a measure of the ES efficiency [1,5]. In the case of Upper Hybrid Resonance (UHR)

$$\omega_i^2=\omega_{pe}^2(x_r)+\omega_{ce}^2(x_r) \quad , \qquad (2)$$

in small-sized plasmas where the density scale length $l << c/\omega_i$, $0 < q < (l\rho_{He}^2)$, I(q) is proportional to q [1]. As is seen from Eq. (1), the ES signal should strongly depend on the resonance position $x_r(\omega_i)$. For harmonic density perturbations $\delta n_\Omega \sim \delta(\Omega-\Omega_0)$, this dependence can be used to reconstruct the spatial distribution of the density perturbation from the interferometer signal $A_{IES}(x_r) = \langle e^{-i\Omega t}A_{ES}(t,x_r)\rangle_t$. The Fourier transform then reads

$$\delta n_{\Omega}(x) \sim N(x) = \int_{-\infty}^{+\infty} \frac{dq}{2\pi q} e^{-iqx} \int_{-\infty}^{+\infty} dx_r e^{iqx_r} A_{IES}(x_r) \quad , \qquad (3)$$

The technique based on this idea is applied in an upper hybrid resonance scattering experiment with tokamak-like magnetic field geometry. The experimental investigations were performed in the laboratory device BOXES [6], in which the inhomogeneous magnetic field was provided by inclination of two magnetic field coils. The effective "tokamak major radius" was R = 70 cm. The plasma was produced by RF pulses capacitively coupled to two grid-plate antennae at the ends of the chamber (f_{RF} = 46 MHz, $P_{RF} \approx$ 325 W, τ_{RF} = 25 μs). The parameters of the helium plasma in the RF pulse were $n_e \leq 4.5 \times 10^{16}$ m^{-3}, $T_e < 4$ eV, and p = 1.25 Pa.

In Fig. 1 (top), we have plotted the normalized plasma density distributions in direction of the magnetic field inhomogeneity measured just after the RF pulse and at the point of time in the afterglow, where the ES measurements were carried out. The LH test wave antenna was placed on the low magnetic field side of the device at x = 9 cm and shifted from the symmetry plane (at z = 0) along the field lines to z = 12 cm. The tokamak scheme of incident wave excitation was used, i.e. microwaves at frequency f_i = 2.45 GHz with power P_i = 100 mW was launched into the plasma from the high magnetic field side. A waveguide serving as transmitting and receiving antenna was located in the equatorial plasma at a radial position x = -4 cm.

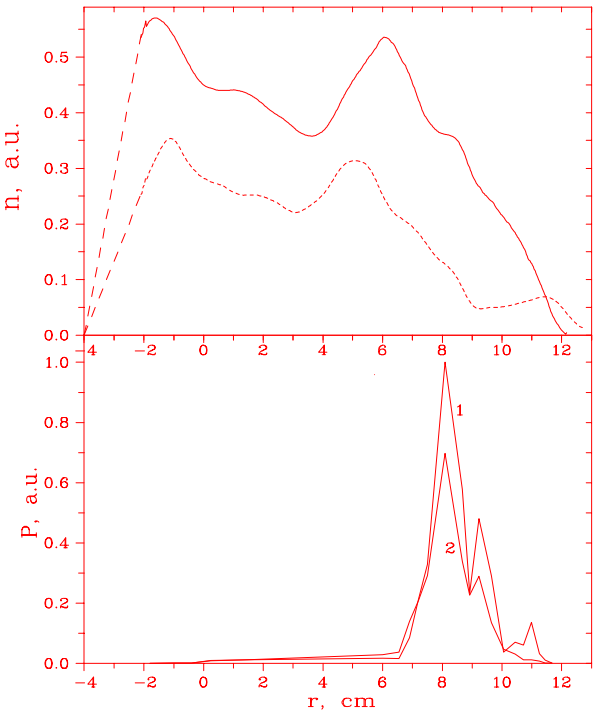

Fig. 1. Top: Density profiles 5 μs after RF pulse without test wave launching (solid line) and 25 μs after RF pulse with test wave launching (dashed line).- Bottom: Internal (nearly isotropic) fluctuations measured by ES 5 μs in the afterglow (Curves 1 and 2 are related to the red and blue part of the spectrum, respectively).

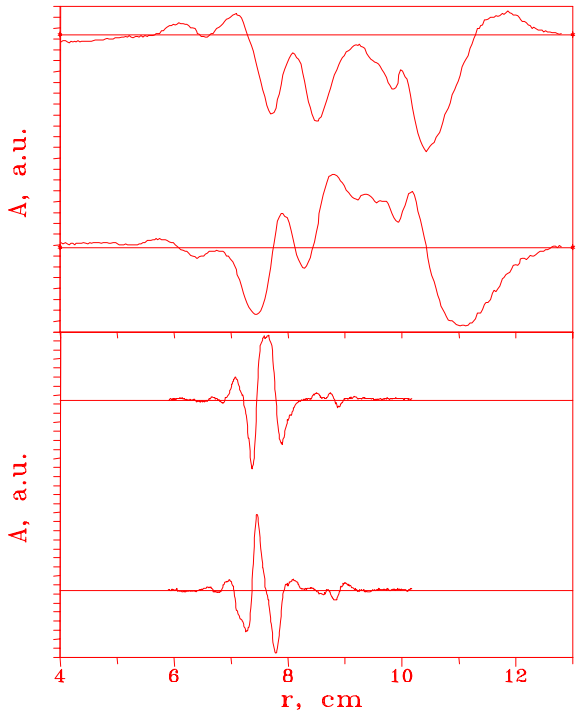

Fig. 2. 0^0 and 90^0 RF probe (top) and ES (bottom) traces taken 25 μs in the afterglow; 0π0π phasing, f_{test} = 23 MHz.

The tokamak-like behavior of the ES signal was checked by backscattering off internal (spontaneously excited) plasma fluctuations in the UHR zone is shown in Fig. 1 (bottom). The spatial scan was performed by variation of the probing frequency making use of the UHR relation (2). The scattered signal was only observed under the condition that the UHR zone exists within the plasma. The maximal values of ES signal were obtained in the range 6 cm < x_r < 10 cm, when the electron cyclotron layer is present inside the plasma and the UHR is accessible. This feature is characteristic for the ES experiment in tokamak geometry.

Typical traces of the IES measurements are shown in Fig. 2 (bottom) with a test wave frequency f_{Test}=23 MHz. For both values of reference signal phase (0^o and 90^o) the interferogram of the wave packet is well localized in the outer part of the gradient region of the density distribution. Contrary to this behavior, the wave packets obtained from the RF probe measurements are much wider and cover the whole gradient region (Fig. 1 (top)).

The Fourier power spectra obtained from these interferograms differ considerably for the RF probe and IES signals (Fig. 3 (top)).

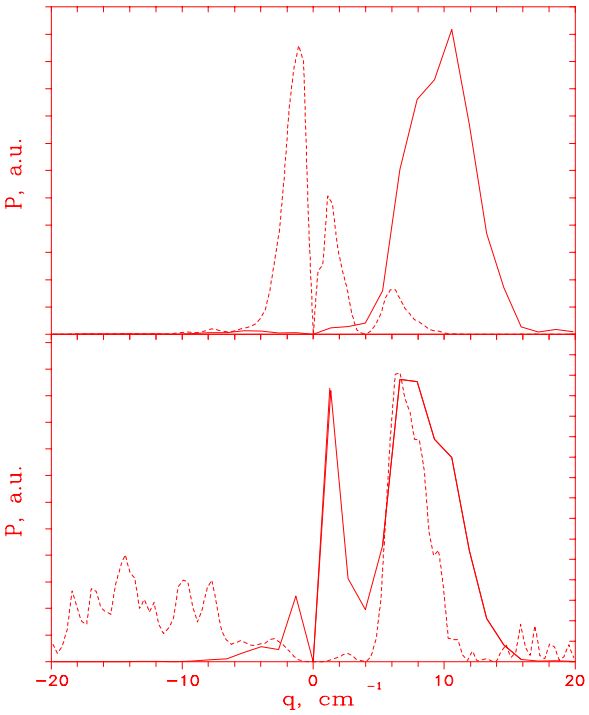

Fig. 3: Top: Original ES (solid line) and RF probe (dashed line) wavenumber spectra.- Bottom: Recalculated ES (solid line) and RF probe (dashed line) wavenumber spectra. Powers weighted with q^{-2} and q^4, respectively.

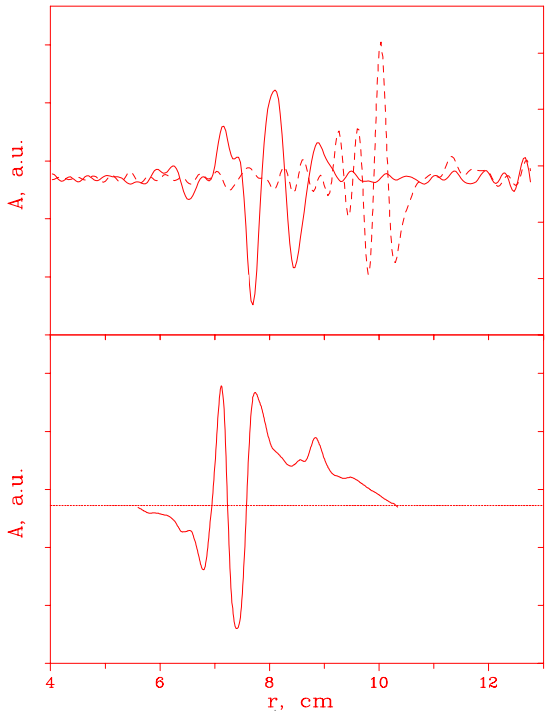

Fig. 4: Top: Solid and dashed packet from positive (red) and negative (blue) part of recalculated RF probe *q*-spectrum, respectively.- Bottom: Reconstructed test wave packet (0^0) from recalculated ES wavenumber spectrum.

That is, the IES spectrum is well localized in the positive q-region and thus corresponds to a wave phase propagating outwards in agreement with the backward behavior of the LH waves. The RF probe spectrum is asymmetric as well, but shifted in negative q-direction. Moreover, the mean q-values turn out to be larger for the ES measurements. The latter discrepancy can be accounted for a different sensitivity of the two diagnostics with respect to the wavenumber.

Namely the RF probe diagnostics measures the plasma potential and is therefore most sensitive to long-scale density perturbations, whereas the IES senses preferably the small scale part of the spectrum, because of the linear q-scaling of the weight function. For a proper comparison the density perturbation spectra were recalculated multiplying the data of Fig. 3 (top) by appropriate weight functions.

From the Poisson equation $\Delta\varphi = -4\pi(\rho_i+\rho_e)$, one can infer that the ratio of density and potential disturbance is q^2 so that the relation $\delta N_{RF} \sim q^2 A_{RF}$ holds, whereas Eq. (1) gives $\delta N_{IES} \sim q^{-1} A_{IES}$. The wavenumber spectra for δN_{RF} and δN_{IES} are shown in Fig. 3 (bottom). It can be seen that the positive q-parts of these spectra are similar, whereas the negative parts are different. The reason for this difference can be understood from Fig. 4 (top) where the spatial distributions $\delta N_{RF}(x)^{q<0}$ and $\delta N_{RF}(x)^{q>0}$ are recalculated using the Fourier spectra. As it is seen from Fig. 4, the position and spatial structure of the density perturbations recalculated from IES data (bottom) coincides with the wave packet calculated from the positive part of the RF probe q-spectrum (top). Both of them are located in the outer part of the gradient region of plasma density profile (Fig. 1 (top)) which is accessible to the probing wave. The negative part of the RF probe q-spectrum is however associated with waves travelling towards the density hump near the plasma edge. This part of plasma is probably not accessible to the incident probing wave, because an evanescence region exist near the minimum of the density profile. This circumstance may explain the suppression of the negative q part in the IES spectrum.

In conclusion, it is emphasized that the first application of Interferometer Enhanced Scattering in a tokamak-like plasma have resulted in measurements of the spatial structure of (externally excited) lower-hybrid waves in good agreement with those obtained with an RF probe technique.

Acknowledgments

The paper was supported by the Deutsche Forschungsgemeinschaft, grants SFB 191 and 146 113/146, RFBR grant 96-02-17913 and Grant supporting Scientific Schools 96-15-96367.

References

[1] Novik K.M. and Piliya A.D.: Plasma Phys. Control. Fusion **35**, 357 (1993).
[2] Arkhipenko V.I. et al.: Plasma Phys. Control. Fusion **37**, A347 (1995).
[3] Arkhipenko V.I., Budnikov V.N., Gusakov E.Z., Selenin V.L. and Simonchik L.V.: Tech. Phys. Lett. **19**, 20 (1993).
[4] Gusakov E.Z., Kaganskaya N.M., Lvov M.V. and Selenin V.L.: Contr. papers ICPP 96, V2, Nagoya 1996
[5] Brüsehaber B., Gusakov E. Z., Krämer M. and Piliya A. D.: Plasma Phys. Control. Fusion **36**, 997 (1994)
[6] Brüsehaber B. and Krämer M.: Plasma Phys. Control. Fusion **39**, 389 (1997)